Progress on NASA NAIRAS Model Development

Christopher J. Mertens[1], John W. Wilson[1], Steve R. Blattnig[1], Brian T. Kress[2], John W. Norbury[1], Michael J. Wiltberger[3], Stan C. Solomon[3], W. Kent Tobiska[4], Joseph Kunches[5], Barbara Grajewski[6], and John J. Murray[1]

[1]NASA Langley Research Center, Hampton, Virginia
[2]Dartmouth College, Hanover, New Hampshire
[3]HAO/NCAR, Boulder Colorado
[4]Space Technologies, Inc., Pacific Palisades, California
[5]NOAA Space Weather Prediction Center, Boulder, Colorado
[6]CDC/NIOSH, Chicago, IL

Space Policy Institute Workshop on Space Weather, Aviation, and Spaceflight
January 11, 2008

Atmospheric Ionizing Radiation
Why the Interest?

- **Source**
  - Galactic Cosmic Rays (GCR) (origins outside the solar system)
  - Solar Energetic Particles (SEP) (origins from solar storm activity)
- **Effect**
  - Primary source of human exposure to radiation with high-LET (linear energy transfer)
  - High-LET radiation is effective at producing chemically active radicals in biological tissues that alter the cell function or result in cell death

Cosmic Ray Interactions

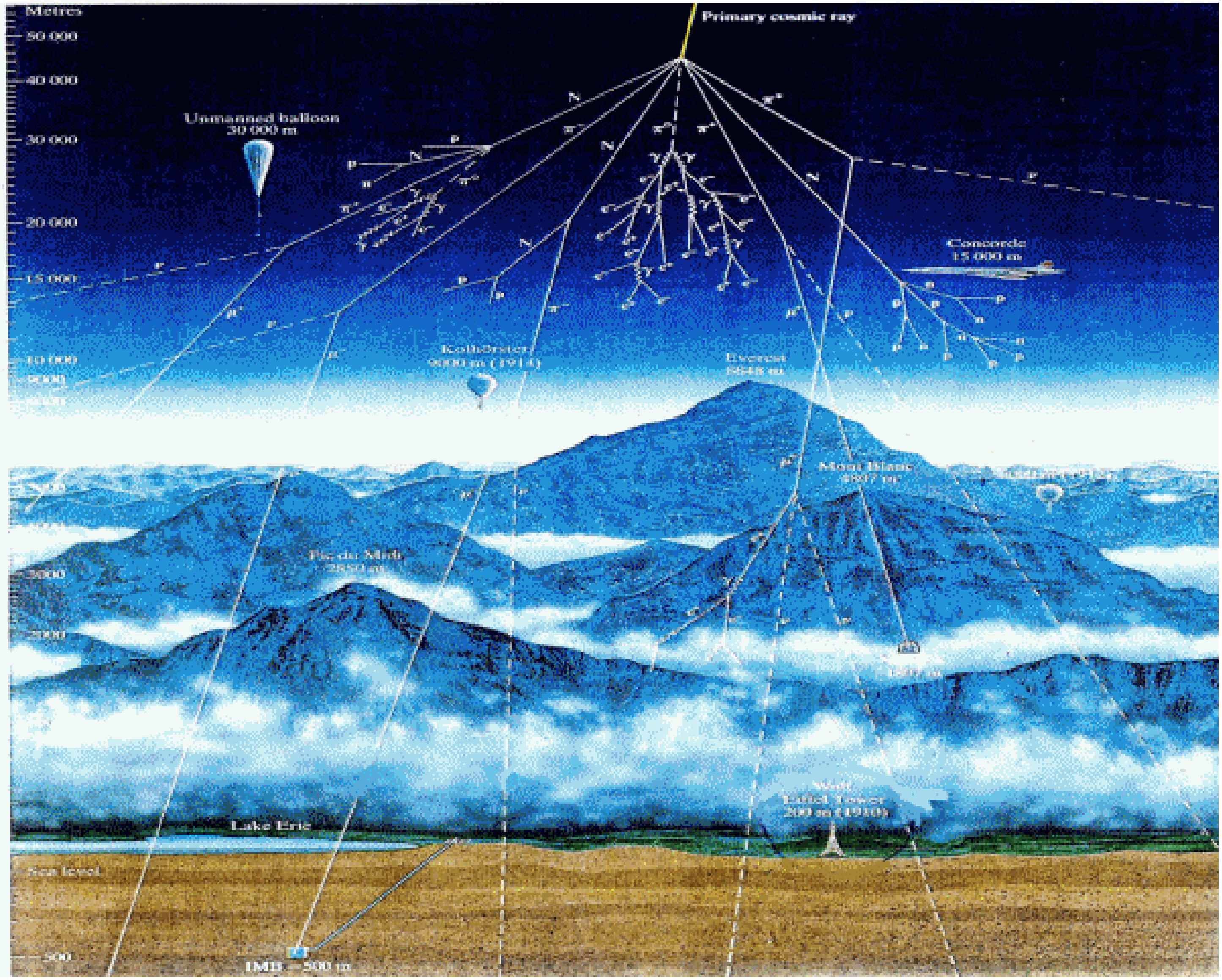

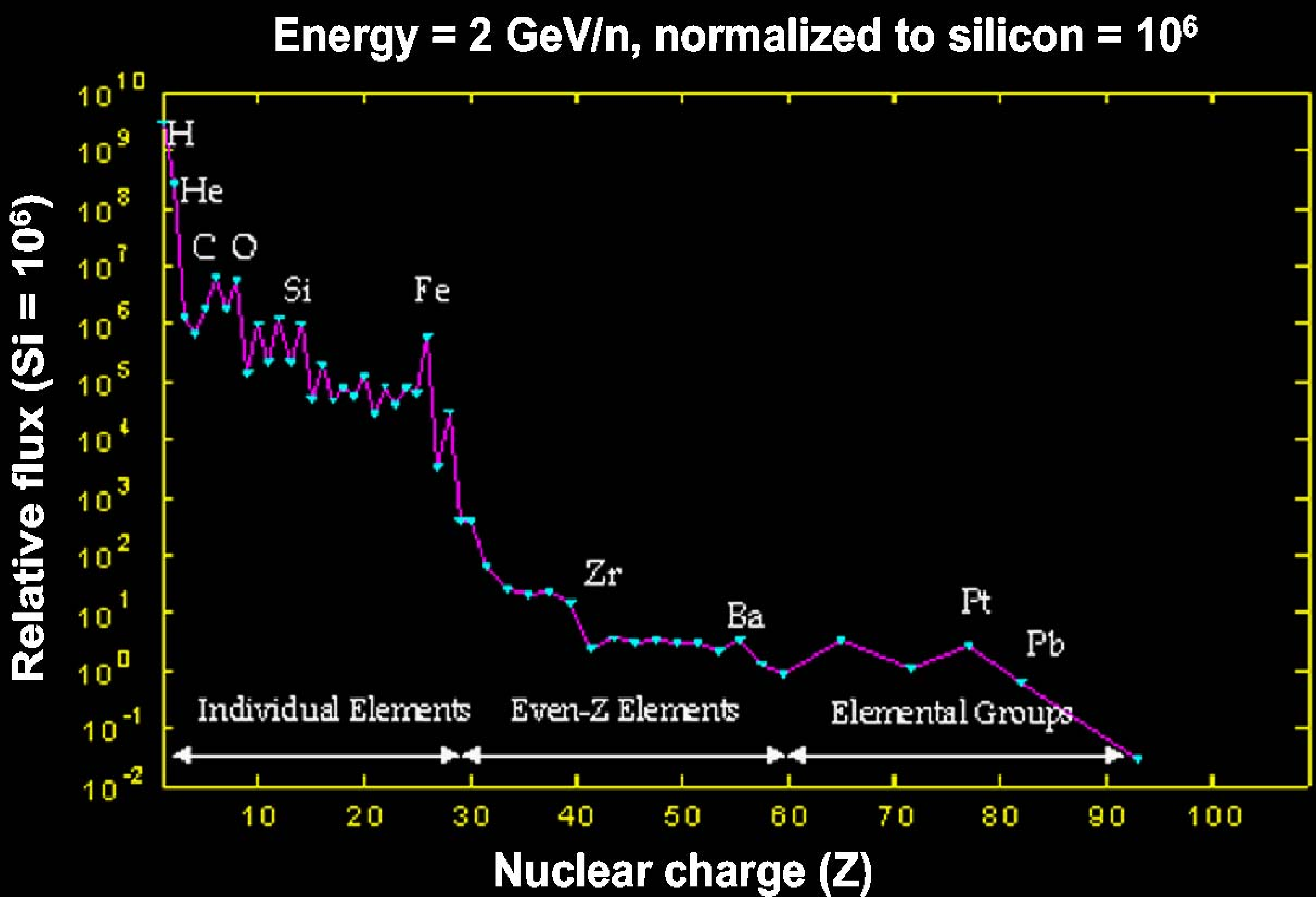

Energy = 2 GeV/n, normalized to silicon = 10^6
Relative flux (Si = 10^6)
Nuclear charge (Z)
H
He
C O
Si
Fe
Zr
Ba
Pt
Pb
Individual Elements
Even-Z Elements
Elemental Groups

Ways to damage DNA

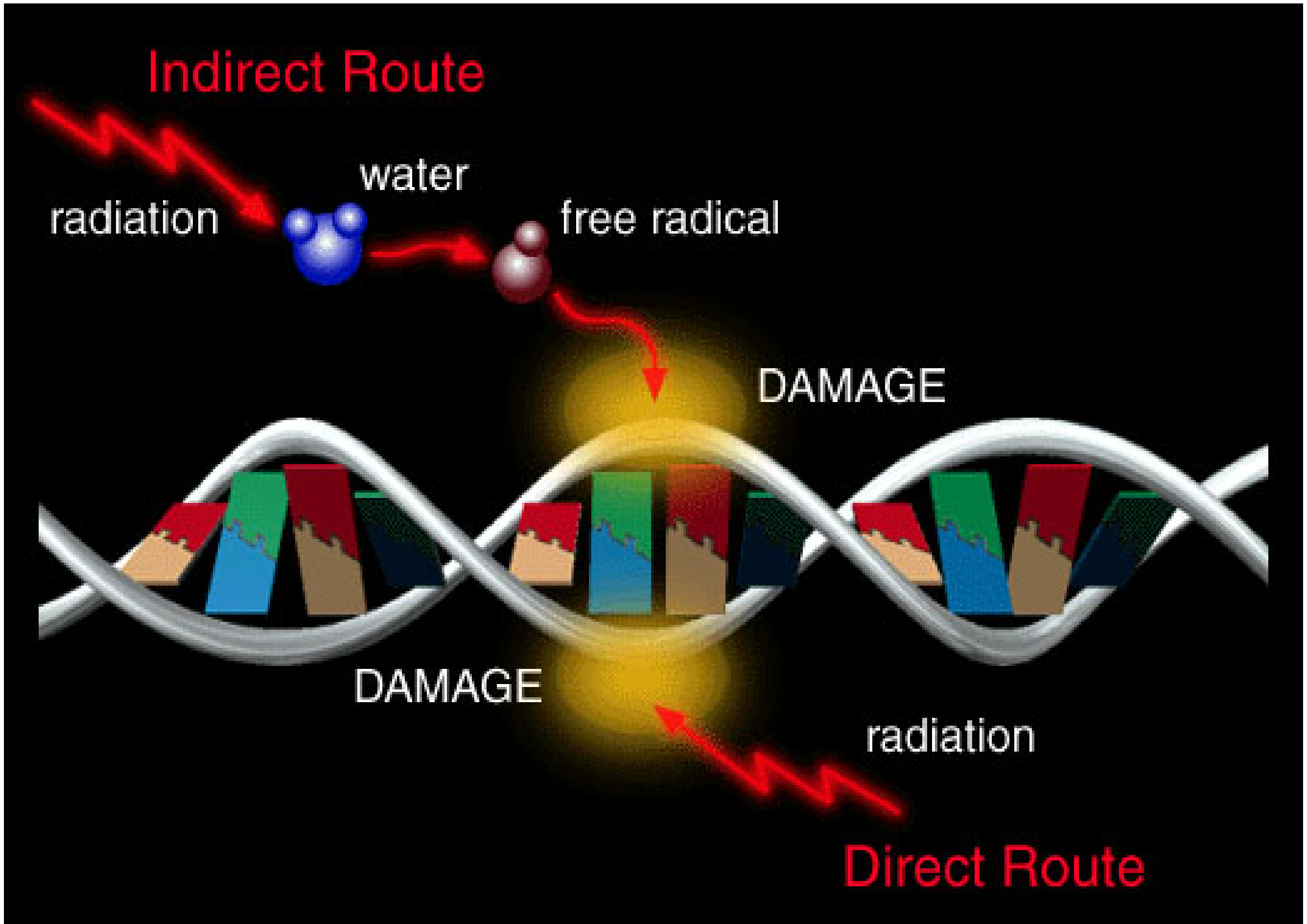

Atmospheric Radiation Transport and Dosimetry

Brief NASA LaRC History

- Foelsche began detailed study of atmospheric ionizing radiation with possible development of HSCT (NASATN D-7715, 1974).
  - Over 300 flight experiments from 1965-1971
  - Theoretical program developed to extend neutron measurement to high-energy
  - Neutrons found to be a major source of radiation exposure at aircraft altitudes
- Conclusions:
  - Exposure at supersonic altitudes is a problem
  - Exposure at subsonic altitudes is within limits for the general populations

Atmospheric Radiation Transport and Dosimetry

Renewed Interest and Concern. Why?

- The highly ionizing components of atmospheric radiations are found to be more biologically damaging than previously assumed.
- The associated relative biological effectiveness for fatal cancer has been increased [*ICRU* 1986; *ICRP* 1991].
- Recent studies on developmental injury in mice embryos indicate large relative biological effectiveness for protection in prenatal exposures [*Jiang et al.,* 1994].
- Flight crews are logging greatly increased hours [*Bramlitt,* 1985; *Wilson and Townsend,* 1988; *Friedberg et al.,* 1989; *Barish,* 1990].
- Airline crew members are now classified as radiation workers [*McMeekin*, 1990; *ICRP* 1991].
- Exponential increase in the number of commercial aircraft polar routes; high-latitudes are the most exposed geographical region [AMS & SolarMetrics Highlights of a Policy Workshop, 2007]

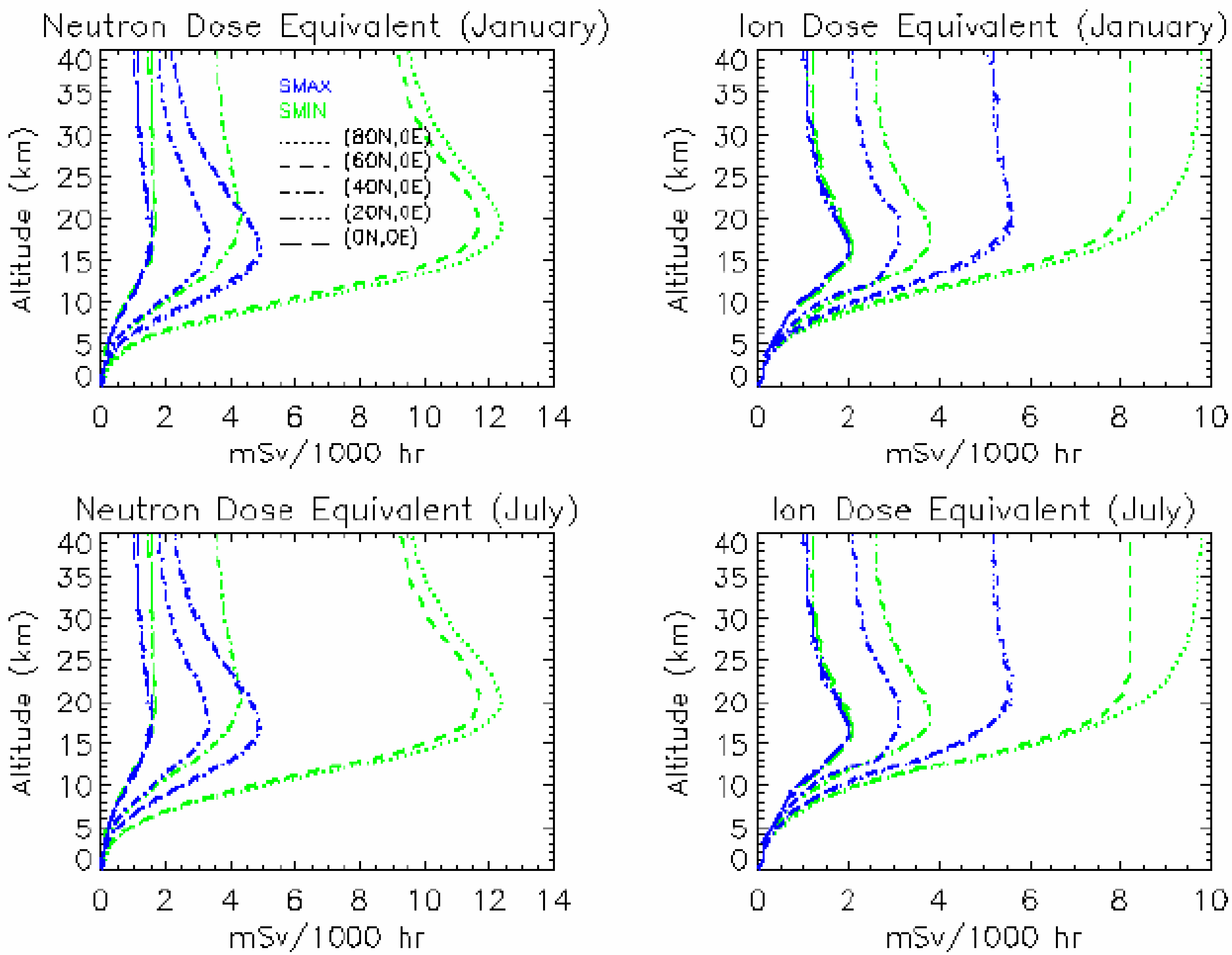

Neutron Dose Equivalent (January)
Ion Dose Equivalent (January)
Neutron Dose Equivalent (July)
Ion Dose Equivalent (July)
SMAX
SMIN
(80N,0E)
(60N,0E)
(40N,0E)
(20N,0E)
(0N,0E)
Altitude (km)
mSv/1000 hr

Units Overview

- Unit of absorbed dose:
  - 1 Gray == 1 J/kg
- Radiation weighting factor: w_R
  - Sievert = Gray x w_R
- ICRP estimate:
  - 1 in 20,000 risk of fatal cancer per 1mSv dose (lifetime).

Radiation Weighting Factors (ICRP publ. 60)

Radiation		w_R
x- & γ-rays, all energies		1
electrons, muons, all energies		1
Neutrons	< 10 keV	5
	10-100 keV	10
	100keV to 2MeV	20
	2 - 20 MeV	10
	> 20 MeV	5
Protons	> 2MeV	5
α, fission fragments, heavy ions		

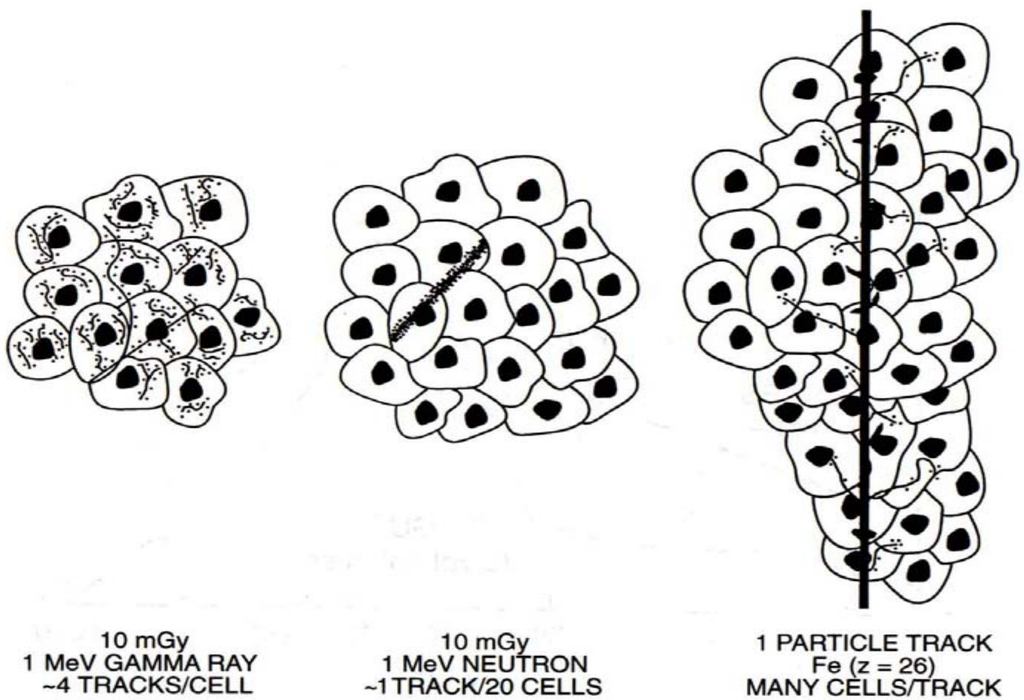

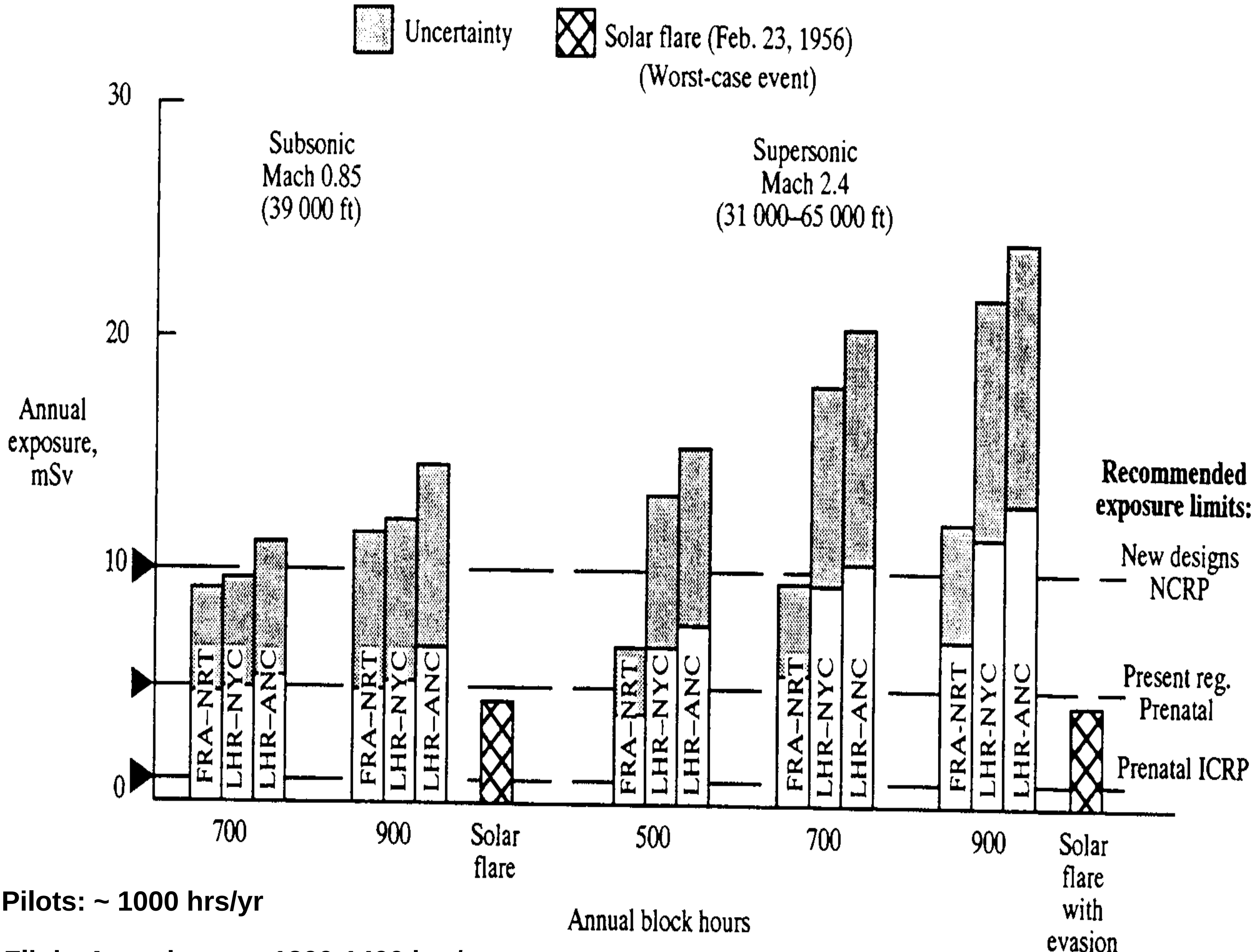

Pilots: ~ 1000 hrs/yr

Flight Attendants: ~ 1300-1400 hrs/yr

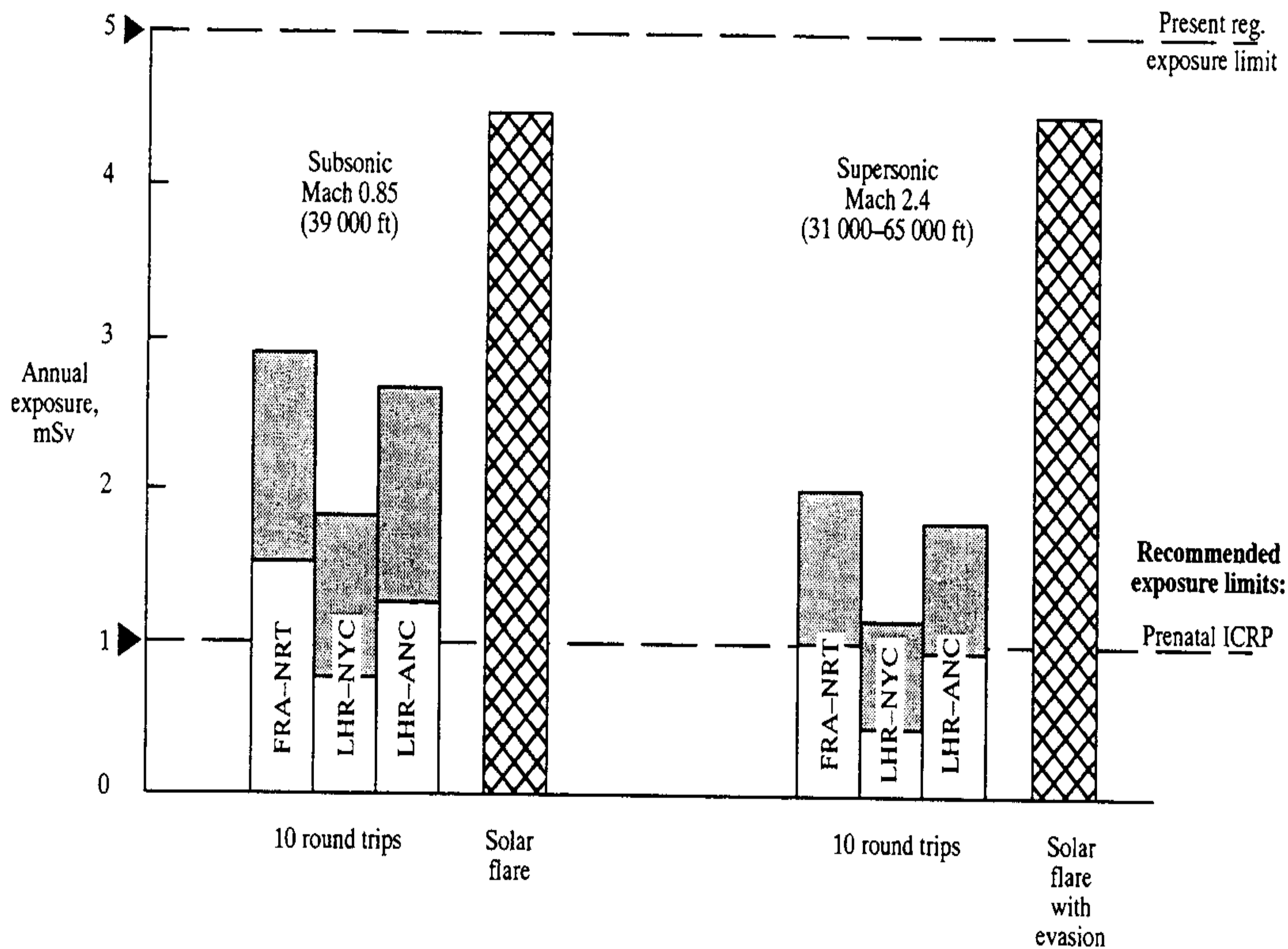

Present reg. exposure limit
5
4
3
2
1
0
Annual exposure, mSv
Subsonic Mach 0.85 (39 000 ft)
Supersonic Mach 2.4 (31 000–65 000 ft)
FRA–NRT
LHR–NYC
LHR–ANC
FRA–NRT
LHR–NYC
LHR–ANC
Recommended exposure limits:
Prenatal ICRP
10 round trips
Solar flare
10 round trips
Solar flare with evasion

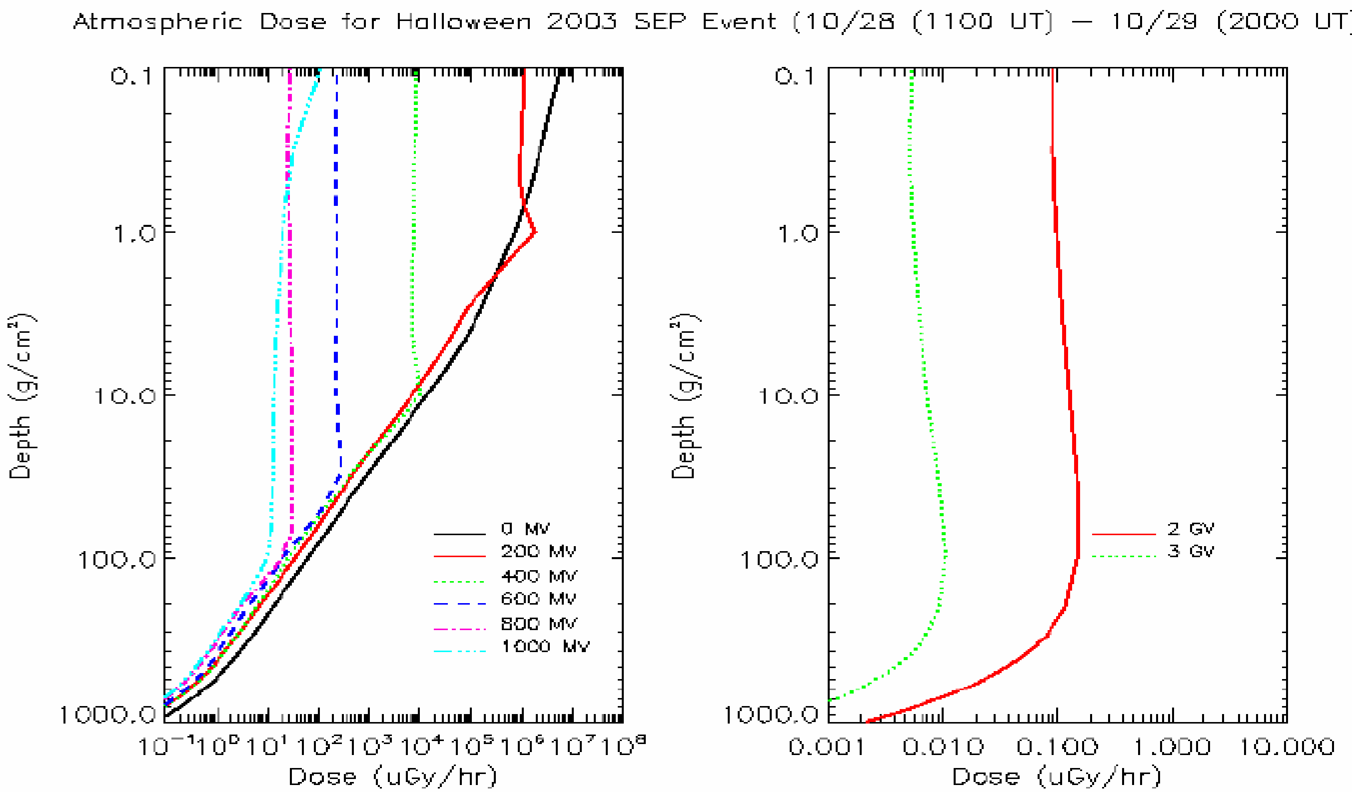

Air dose rates as a function of atmospheric depth for a SEP event (10/28 (11:00 UT) – 10/29 (20:00 UT)) during the Halloween 2003 superstorm event. The left panel shows the atmospheric dose rates for various geomagnetic cutoff rigidities from zero (polar region) to 1 GV. The right panel shows does rates for 2 and 3 GV cutoffs.

Influence of Magnetospheric Current Sources

Magnetic storms can suppress the geomagnetic cutoff rigidity by ~ 1 GV in the region of US international flights for moderate magnetic storms

- **Significant increase in dose in this region**
- **Mid-latitudes regions can be susceptible to the same radiation dose levels as the high-latitude and polar region**

Physics-Based Atmospheric Ionizing Radiation Dosimetry

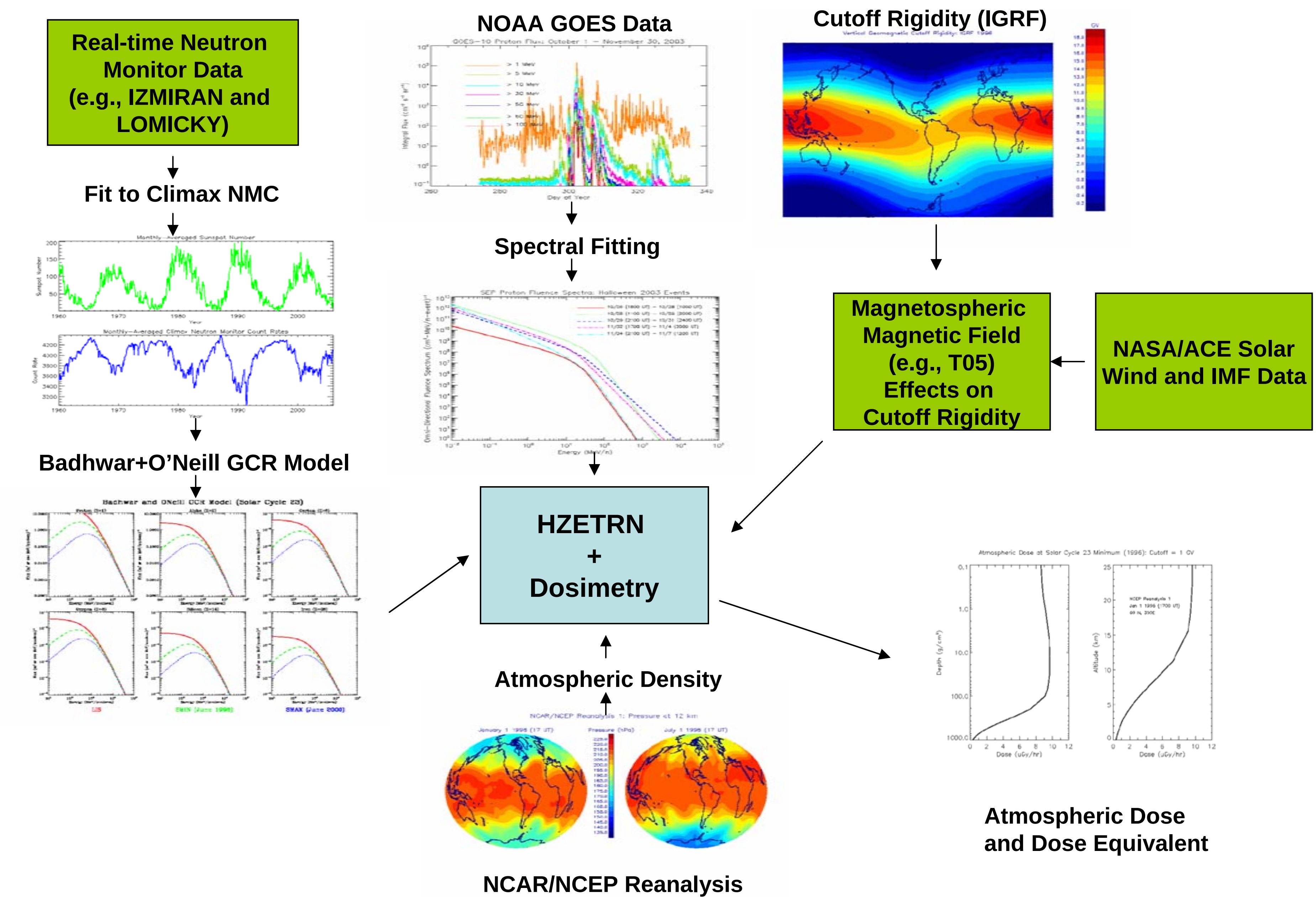

NASA NAIRAS Model (PI: Christopher J. Mertens)

Earth System Models

Radiation Dose Rates:

AIR (parametric)

HZETRN (physics-based)

Near-Earth Space Environment

•Badhwar/O'Neill GCR Model

•Empirical Cutoff Rigidity

(IGRF+T05)

•Physics-based Cutoff Rigidity

(LFM/CMIT+SEP-trajectory)

Earth Observations

Near-Earth Space Environment

NASA/ACE

NASA/HEAO-3

NOAA/GOES

Assimilated Atmospheric

Atmospheric Depth (NCAR/NCEP)

Ground-Based

Neutron Count Monitors

Predictions/Forecasts

Ionizing Radiation Nowcast

3-D Dose Equivalent

3-D Differential Flux

NAIRAS Distributed Network System

High-Performance Computer Systems

Server Interface

Operational and Archival

Databases

Differential Particle Flux

HZE Particles (Z=5-26)

Light-Ions (Z=1-4)

Neutrons

Pions and Muons

Electromagnetic Cascasde Particles

Observations, Parameters & Products

Decision Support Systems, Assessments, Management Actions

NAIRAS decision support tool for NOAA/SEC space weather forecasts, warnings, and advisories

NAIRAS available at NOAA/ADD experimental aviation-related weather forecasts, observations, and analysis

Specific analyses to support the decision making

Predict real-time radiation exposure at commercial airline altitudes (includes background GCR and SEP events)

Provide accumulated radiation exposures for representative set of domestic, international, and polar routes

Specific Decisions / Actions

Limit aircrew flight hours to within recommended annual and career limits

Alter route and/or altitude during SEP events

Value & Benefits to Society

Improvements in the decision-making, decisions, and actions

First-ever, data-driven, real-time prediction of biologically harmful radiation exposure levels at commercial airline altitudes

Quantitative and qualitative benefits from the improved decisions

Comprehensive database of radiation dose rates to formulate recommended annual and career limits to ionizing radiation exposure

Comprehensive database of radiation dose rates for airlines to assess cost/risk of polar routes

Real-time prediction of radiation exposure levels to enable optimal balance between airline cost and air traveler health risk during solar storm (SEP) events

Improve understanding of biological effects of atmospheric ionizing radiation on aircrew and passengers through collaboration of epidemiological studies by NIOSH

Atmospheric Ionizing Radiation Estimates
Current Status

- **NOAA Space Weather Prediction Center Products**
  - **Does not include nowcast/forecasts of (biological) radiation dose**
- **FAA CARI-6 Web interface**
  - **Includes GCR radiation dose for specified trajectories**
  - **Does not include**
    - **Global coverage**
    - **Real-time assessment**
    - **SEP events**
    - **Storm-time perturbations to geomagnetic cutoff rigidity**
    - **Not physics-based**

Nowcast of Atmospheric Ionizing Radiation for Aviation Safety
NAIRAS Unique Features

- Global
  - Geographic coverage: pole-to-pole
  - Altitude converge: Surface to 100 km
- Real-time
  - 1-3 hr
- Data-Driven
  - Solar-Cycle GCR Modulation: Ground-based neutron monitors
  - SEP spectra: NOAA/GOES
  - Geomagnetic storm effects on cutoff rigidity: NASA/ACE solar wind measurements
  - Atmospheric density: NCAR/NCEP Reanalysis (4x daily)
- Physics-based transport and dosimetry
  - High Charge and Energy Transport (HZETRN) Model
- Both GCR and SEP biological dose predictions

Summary and Conclusions

- **NAIRAS Will Provides New and Significant Contributions**
  - **Provide continuous assessment of the background atmospheric ionizing radiation dose**
    - **Track individual aircrew exposure levels**
    - **Provide airlines and FAA necessary data to develop policies and procedures for aircrew recommended radiation exposure limits and exposure mitigation**
  - **Provide time-critical data during SEP events**
    - **Critical data for airline management and pilots to make decisions concerning flight path alternations**
    - **Enable airlines and pilots to balance the cost of flight path alterations against minimizing radiation exposure and health risks to passengers and crew**
  - **Provide archived database of radiation exposure levels**
    - **Assess the impact of atmospheric ionizing radiation on the global air transportation system**
    - **Assess impact (cost versus health risk) of current and future exponential increase in the number of polar routes**

Summary and Conclusions

- Progress in NAIRAS Model Development
  - Parametric AIR model updated to interface with state-of-the-art specification of GCR solar cycle modulation, geomagnetic cutoff rigidity, and atmospheric density
  - HZETRN configured for global, real-time, data-driven atmospheric ionizing radiation and dosimetry calculations
  - Critical improvements to nuclear cross sections which impact atmospheric neutron and meson-muon transport
  - Progress in understanding the influence of magnetospheric effects on geomagnetic cutoff rigidities and their subsequent impact on atmospheric ionizing radiation dose

Summary and Conclusions

- **Future Efforts**
  - **Model integration**
    - **Complete input data integration with parametric AIR**
    - **Continue to Integrate real-time input models and data sources with HZETRN**
    - **Integrate MESTRN with HZETRN**
    - **Integrate electromagnetic cascade interactions and transport with HZETRN**
  - **Transport physics and interaction processes**
    - **Improve forward and backward neutron transport in HZETRN**
    - **Continue to improve hadron production cross section in HZETRN**
  - **Magnetospheric effects on geomagnetic cutoff rigidities**
    - **Continue to characterize these effects during both quiescent and storm periods**
    - **Develop requirements and algorithm for real-time geomagnetic cutoff rigidity storm model**
  - **Verification and validation**
    - **Assemble ground-level, atmospheric, and space-based measurements to characterize and reduce uncertainties in each component of NAIRAS**
  - **Beyond NAIRAS**
    - **Collaborate with CISM to incorporate SEP forecast capability**

For more information contact:

Dr. C.J. Mertens
NASA Langley Research Center
Hampton, VA 23681
(757) 864-2179
Christopher.J.Mertens@nasa.gov

Back-up Slides follow

Global distribution of dose equivalent rate (mSv/1000 hr) predicted by the parametric AIR model at 12 km for solar maximum conditions (year 2000) of cycle 23.

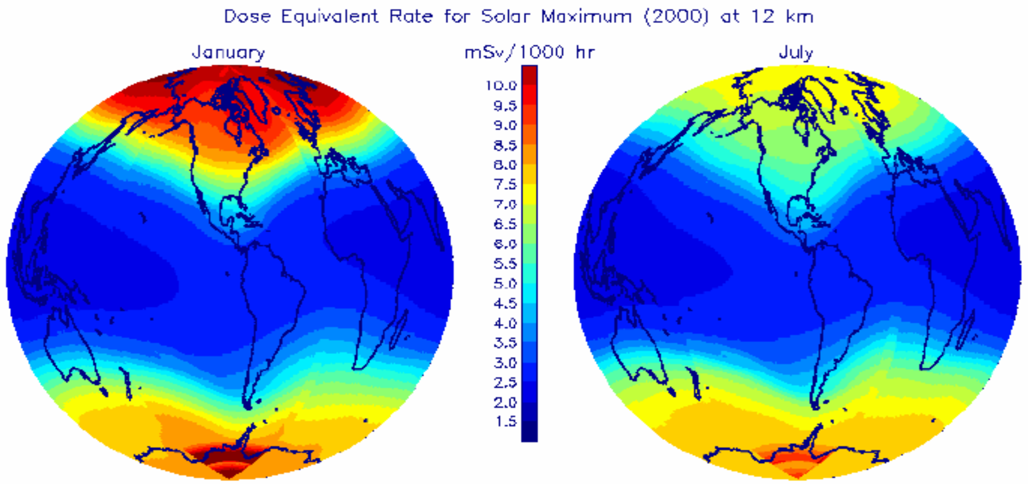

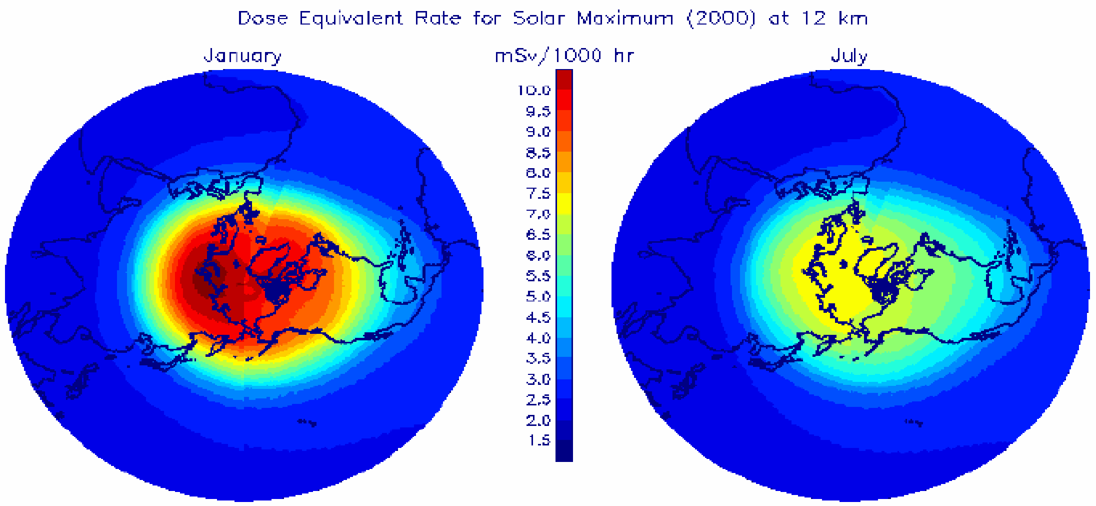

Aircrew logging 1000-hours on high-latitude flights can reach ~ 70% of recommended NCRP annual dose limit

Global distribution of dose equivalent rate (mSv/1000 hr) predicted by the parametric AIR model at 12 km for <u>solar minimum</u> conditions (year 1996) of cycle 23.

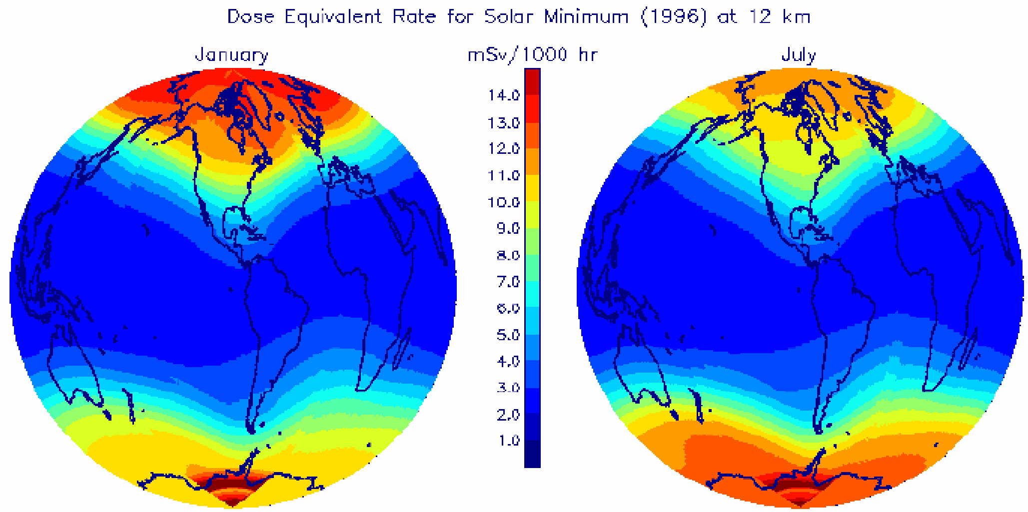

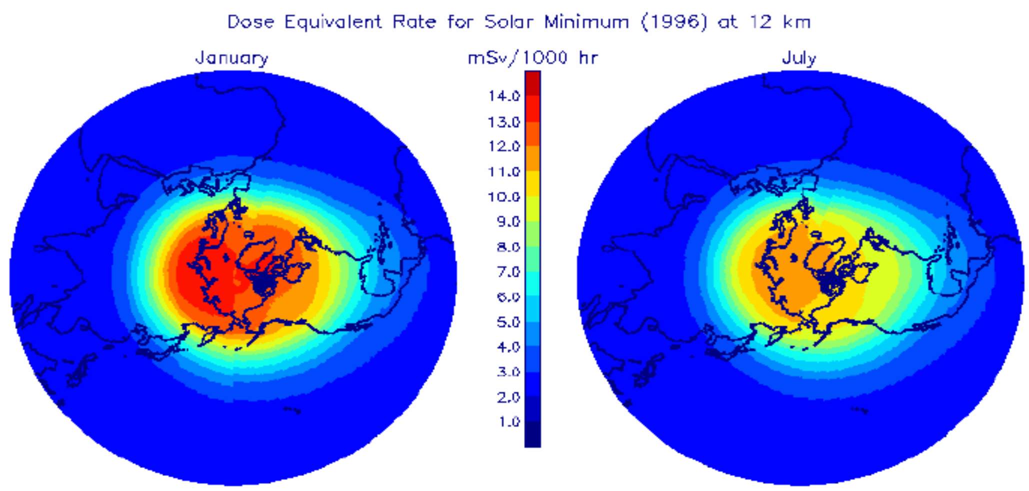

Aircrew logging 1000-hours on high-latitude flights can exceed recommended NCRP annual dose limit

Atmospheric Radiation Transport and Dosimetry

Atmospheric Interactions and Transport

- GCR/SEP Transport
  - HZETRN (physics-based)
  - AIR model (Parametric-GCR)
- HZETRN Code
  - HZE (High Charge and Energy) Particle Transport (Wilson et al., NASA/TP-1995-3495)
  - Coupled Nucleon (Light-Ion+High-Energy Neutron) Transport (BRYNTRN Code: Wilson et al., NASA/TP-1989-2887)
  - Low Energy Neutron Transport (Heinbockel et al., NASA/TP-2000-209865)
  - Meson-Muon Transport (MESTRN Code: Blattnig et al., NASA/TM-2004-212995)
  - Beam Broadening and Transport due to Multiple Coulomb Scattering (Mertens et al., Adv. Space Res., doi:10.1016/j.asr.2007.03.075, 2007)

Methods for Solving for the Fluence Spectra $\phi_j(x,\Omega,E)$

HZE Transport: Linear Boltzmann Equation

$$\mathbf{\Omega} \bullet \nabla \Phi_j(\mathbf{x}, \mathbf{\Omega}, E) = \sum_k \int \sigma_{jk}(\mathbf{\Omega}, \mathbf{\Omega}', \mathrm{E}, \mathrm{E}')\Phi_k(\mathbf{x}, \mathbf{\Omega}', E')d\mathbf{\Omega}'dE' - \sigma_j(E)\Phi_j(\mathbf{x}, \mathbf{\Omega}, E),$$

Total Cross Section

$$\sigma_j(E) = \sigma_{j,at}(E) + \sigma_{j,el}(E) + \sigma_{j,r}(E)$$

$\sigma_{j,at}(E) \sim 10^{-16}\ \mathrm{cm}^{-2};\ \Delta E_{at} \sim 10^{2}\ \mathrm{eV}$ **Atomic: Ion-Electron Scattering**

$\sigma_{j,el}(E) \sim 10^{-19}\ \mathrm{cm}^{-2};\ \Delta \mathrm{E}_{el} \sim 10^{6}\ \mathrm{eV}$ **Elastic Nucleon Scattering**

$\sigma_{j,r}(E) \sim 10^{-24}\ \mathrm{cm}^{-2};\ \Delta \mathrm{E}_{r} \sim 10^{8}\ \mathrm{eV}$ **Nuclear Reactions**

HZETRN GCR Atmospheric Transport

- **Incident GCR spectra: Badhwar and O'Neill Model**

$$j_{LIS}(E) = j_o \beta^{\delta} (E + E_o)^{-\gamma}$$

$$k(r,t) = (k_o / V_{SW}) \beta R \left[1 + (r / r_o)^2 \right] / \Phi(t)$$

  - Solution of steady-state Fokker-Planck equation
  - Proton, Alpha spectra fit to IMP-8 data
  - Lithium-Nickel (Z=3-28) fit to NASA/ACE/CRIS (50-500 MeV/n)
  - High-Energy spectra (1-35 GeV) fit to NASA/HEAO-2 data
  - Reference modulation parameter fit to ACE/CRIS oxygen spectra
  - Subsequent modulation parameter fit to neutron monitor data

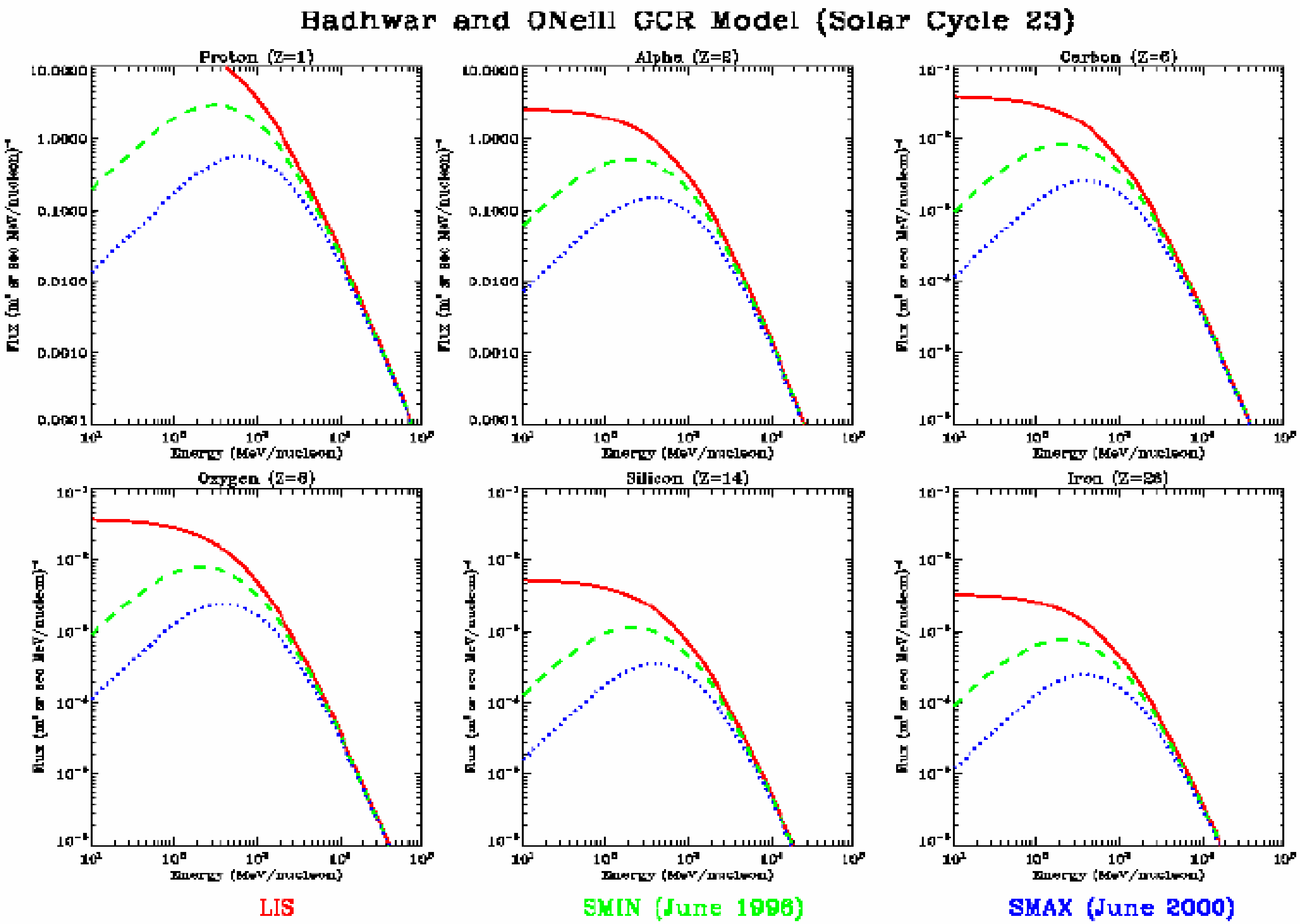

GCR spectral flux for various nuclei predicted by the Badhwar and O'Neill model for solar cycle 23. The local interstellar spectrum (LIS) is denoted by the red lines. Solar minimum spectra are represented by June 1996 conditions, and are denoted by green lines. Solar maximum spectra are represented by June 2000 conditions, and are denoted by blue lines.

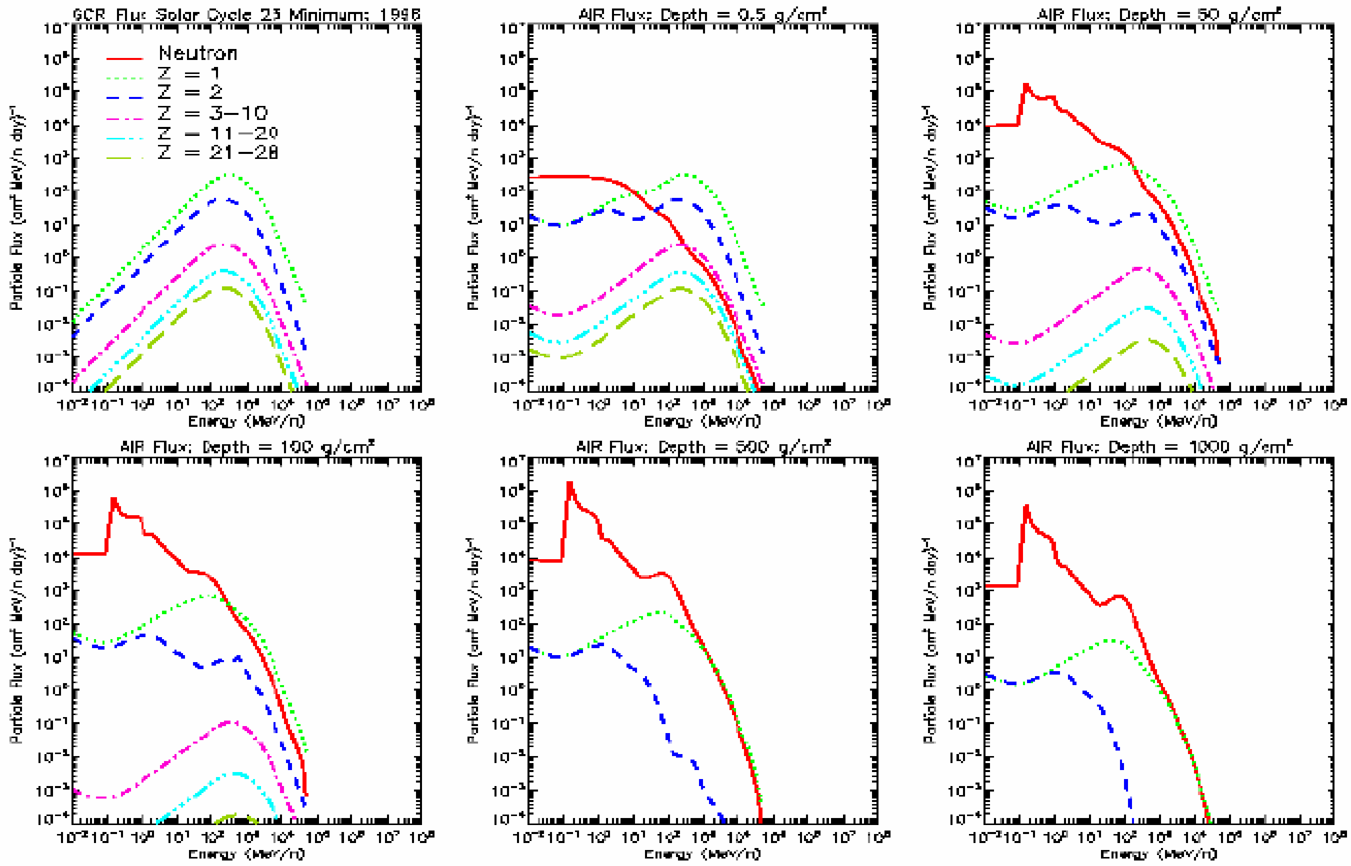

Atmospheric transport of GCR primary and secondary particle spectra computed by HZETRN for zero geomagnetic cutoff rigidity. The top left panel is the 1996 yearly-averaged incident GCR spectrum for solar cycle 23 minimum conditions. The particle flux for various charges have been summed together to reduce the number of line curves. The remaining panels show the GCR spectra at various atmospheric depths.

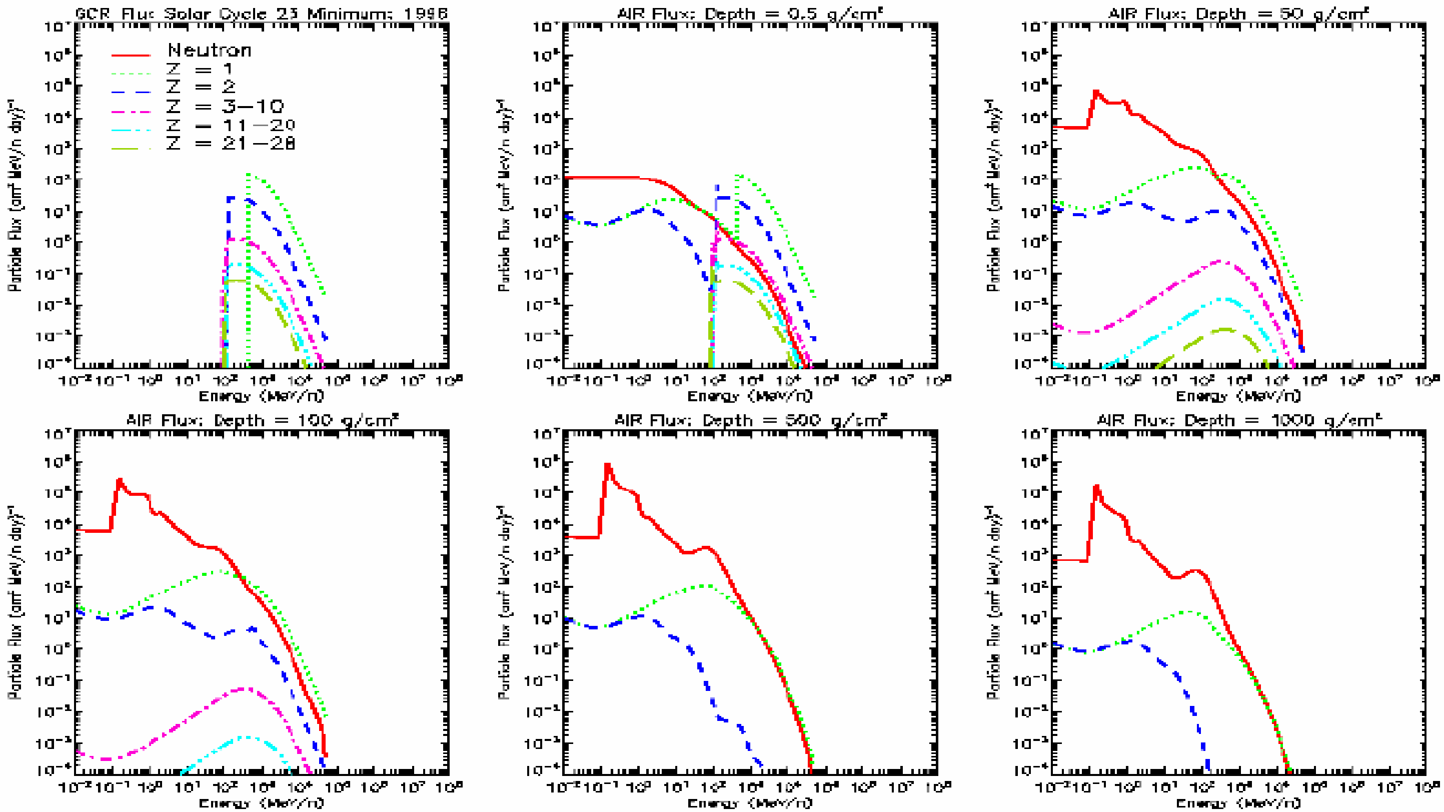

Atmospheric transport of GCR primary and secondary particle spectra computed by HZETRN for 1 GV geomagnetic cutoff rigidity. The top left panel is the 1996 yearly-averaged incident GCR spectrum for solar cycle 23 minimum conditions. The particle flux for various charges have been summed together to reduce the number of line curves. The remaining panels show the GCR spectra at various atmospheric depths.

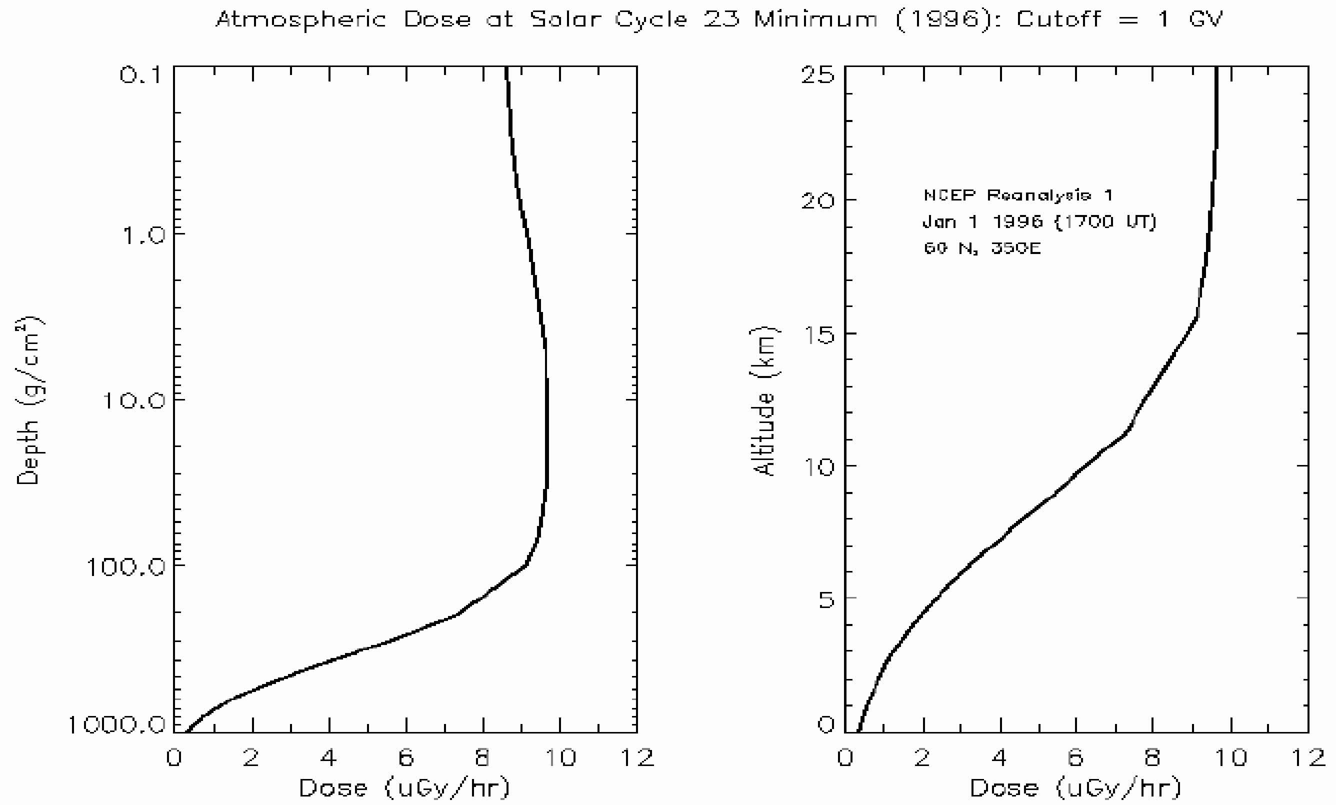

Atmospheric dose (uGy/hr) computed for yearly-averaged incident GCR spectra in 1996, corresponding to solar minimum conditions for cycle 23. The geomagnetic cutoff rigidity was taken to be 1 GV. The left panel shows dose as a function of atmospheric depth (g/cm2). The right panel shows the dose profile mapped from atmospheric depth to altitude (km) using NCEP Reanalysis 1 geopotential height data at 60N, 350E on January 1, 1996 at 17:00 UT.

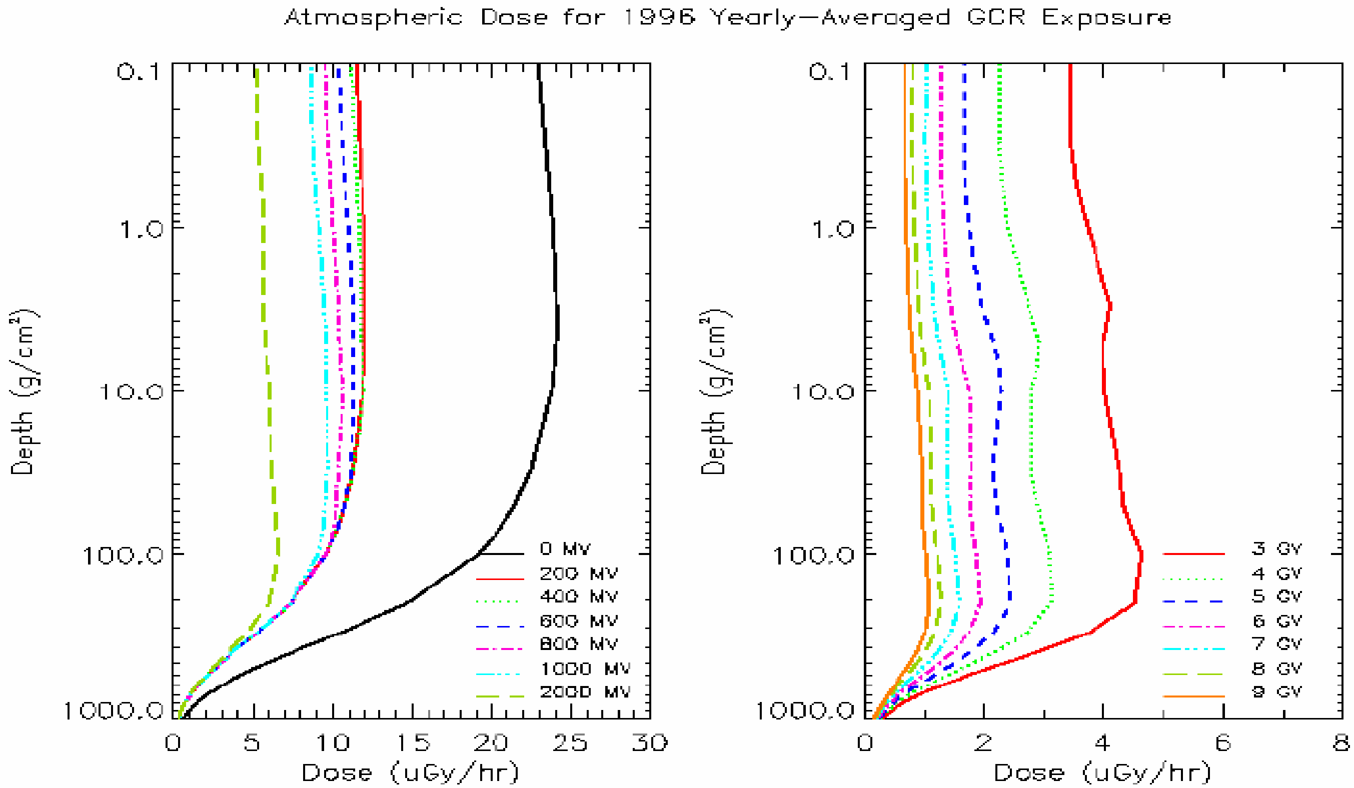

Air dose rates as a function of atmospheric depth for yearly-averaged GCR exposure during solar minimum conditions of cycle 23 (1996). The left panel shows the atmospheric dose rates for various geomagnetic cutoff rigidities from zero (polar region) to 2 GV. The right panel shows does rates for 3-9 GV.

HZETRN SEP Atmospheric Transport

- Incident SEP spectra: non-linear least-squares spectral fit to NOAA/GOES
- Double power-law spectrum [Mewaldt, 2003]

$$dJ/dE = CE^{-\gamma_a} \exp(-E/E_0) \text{ for } E \leq (\gamma_b - \gamma_a)E_0$$

$$dJ/dE = CE^{-\gamma_b} \left\{ \left[(\gamma_b - \gamma_a)E_0 \right]^{(\gamma_b - \gamma_a)} \exp(\gamma_a - \gamma_b) \right\} \text{ for } E > (\gamma_b - \gamma_a)E_0,$$

GOES/SEM EPS and HEPAD channels used to derive proton and alpha fluence spectra

Particle	Channel Designation	Energy Range (MeV)	Instrument
Proton	P2	4-9	EPS (differential)
Proton	P3	9-15	EPS (differential)
Proton	P4	15-40	EPS (differential)
Proton	P5	40-80	EPS (differential)
Proton	P6	80-165	EPS (differential)
Proton	P7	165-500	EPS (differential)
Proton	P8	350-420	HEPAD
Proton	P9	420-510	HEPAD
Proton	P10	510-700	HEPAD
Proton	I3-I2	5-10	EPS (>10 - >5)
Proton	I4-I3	10-30	EPS (>30 - >10)
Proton	I5-I4	30-50	EPS (>50 - >30)
Proton	I6-I5	50-60	EPS (>60 -> 50)
Proton	I7-I6	60-100	EPS (>100 - >60)
Alpha	A1	4-10	EPS (differential)
Alpha	A2	10-21	EPS (differential)
Alpha	A3	21-60	EPS (differential)
Alpha	A4	60-150	EPS (differential)
Alpha	A5	150-250	EPS (differential)
Alpha	A7	2560-3400	HEPAD

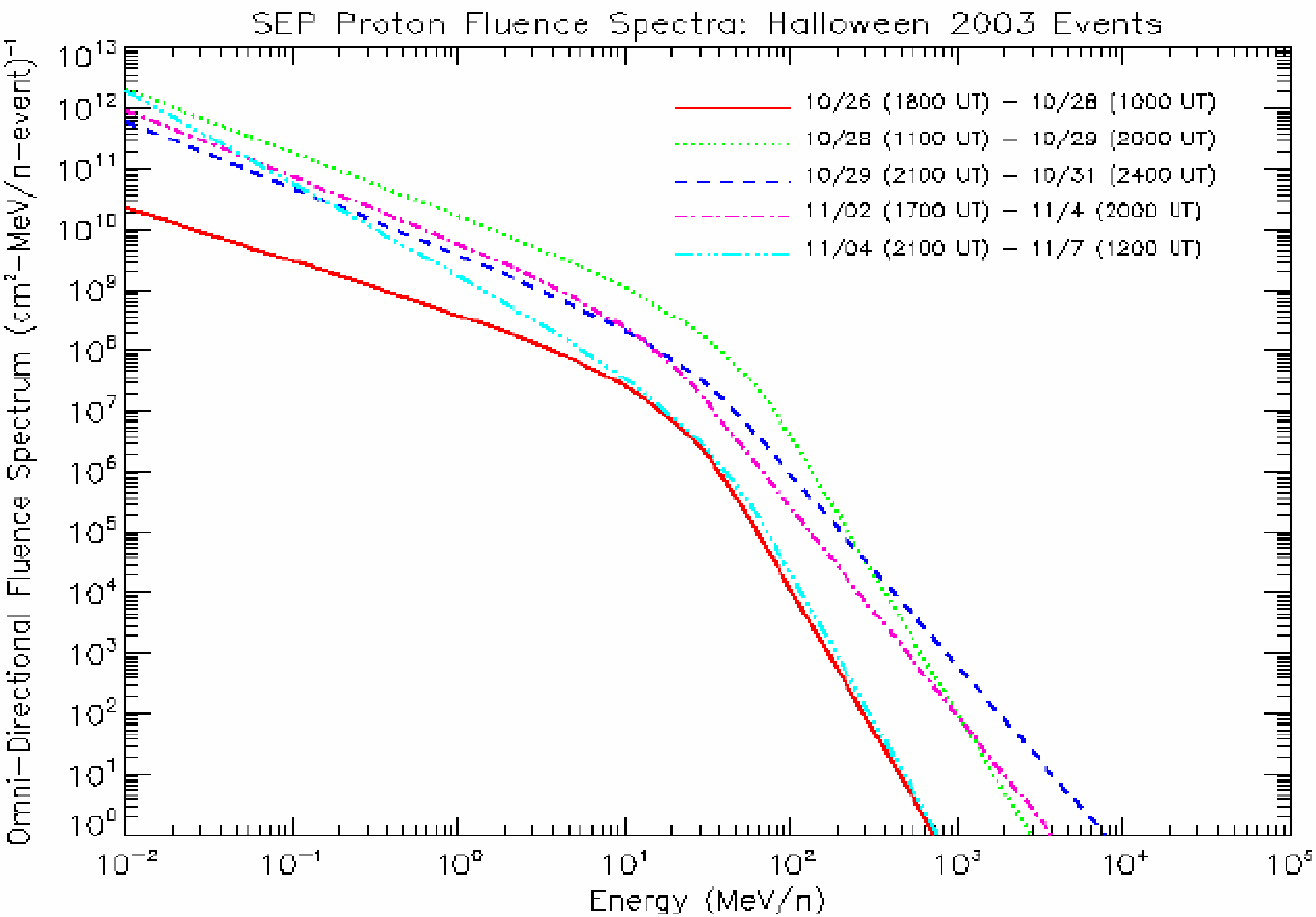

Proton fluence spectra for five SEP events during the Halloween (October-November) 2003 superstorm event.

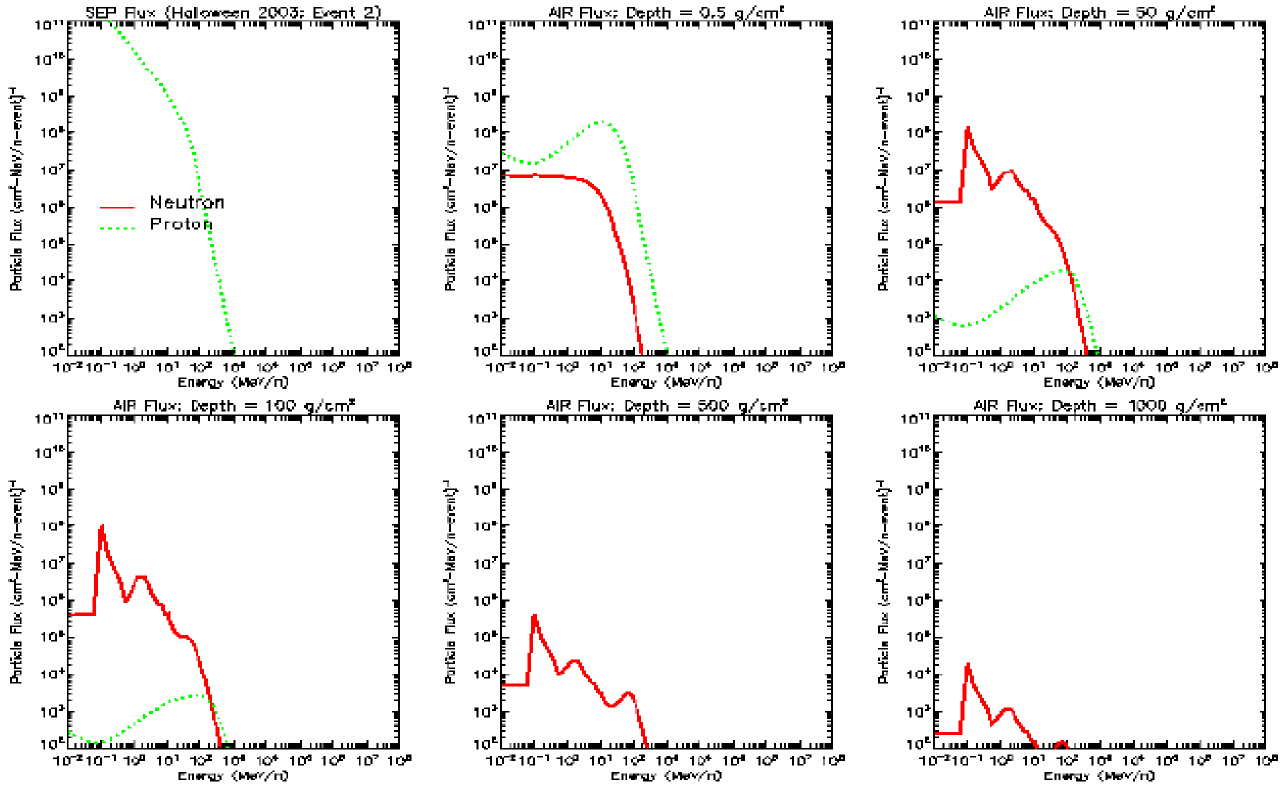

Atmospheric transport of SEP primary and secondary particle spectra computed by HZETRN for zero geomagnetic cutoff rigidity. The top left panel is the incident SEP proton spectrum for event 2 (10/28 (1100 UT) – 10/29 (2000 UT) of the Halloween 2003 storm shown in Figure 19. The remaining panels show the proton and neutron spectrum at various atmospheric depths.

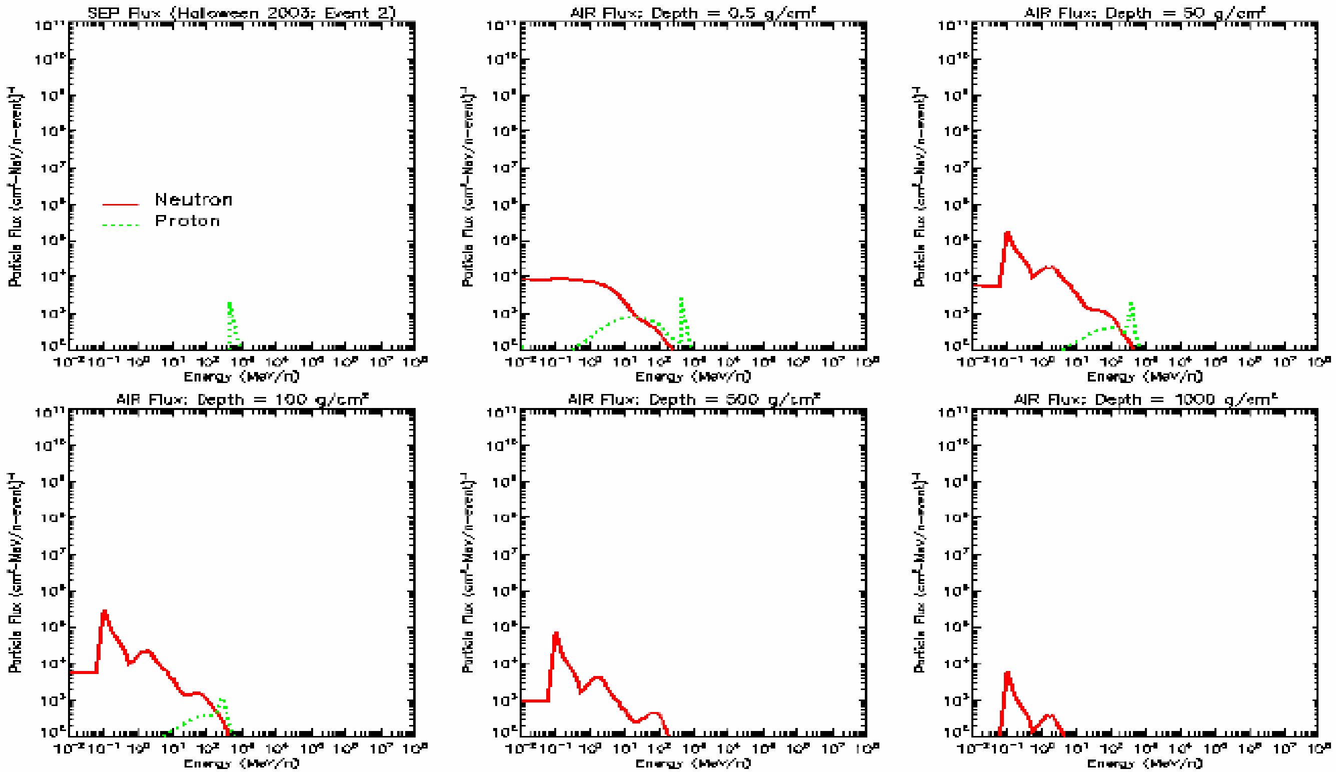

Atmospheric transport of SEP primary and secondary particle spectra computed by HZETRN for 1 GV geomagnetic cutoff rigidity. The top left panel is the incident SEP proton spectrum for event 2 (10/28 (1100 UT) – 10/29 (2000 UT) of the Halloween 2003 storm shown in Figure 19. The remaining panels show the proton and neutron spectrum at various atmospheric depths.

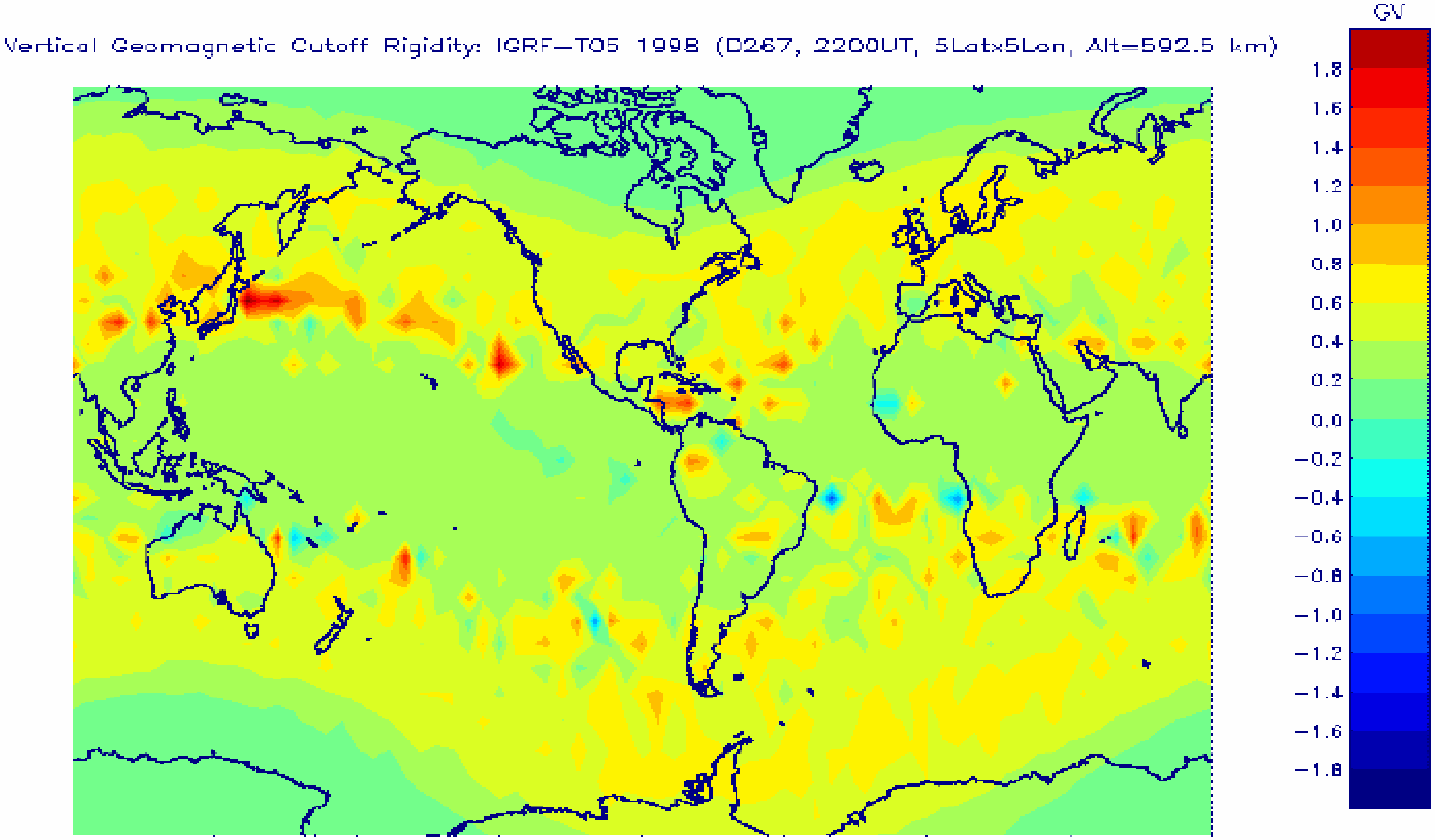

Vertical geomagnetic cutoff rigidity difference (GV) at 22:00 UT on September 24, 1998 using different magnetic field models: IGRF-T05

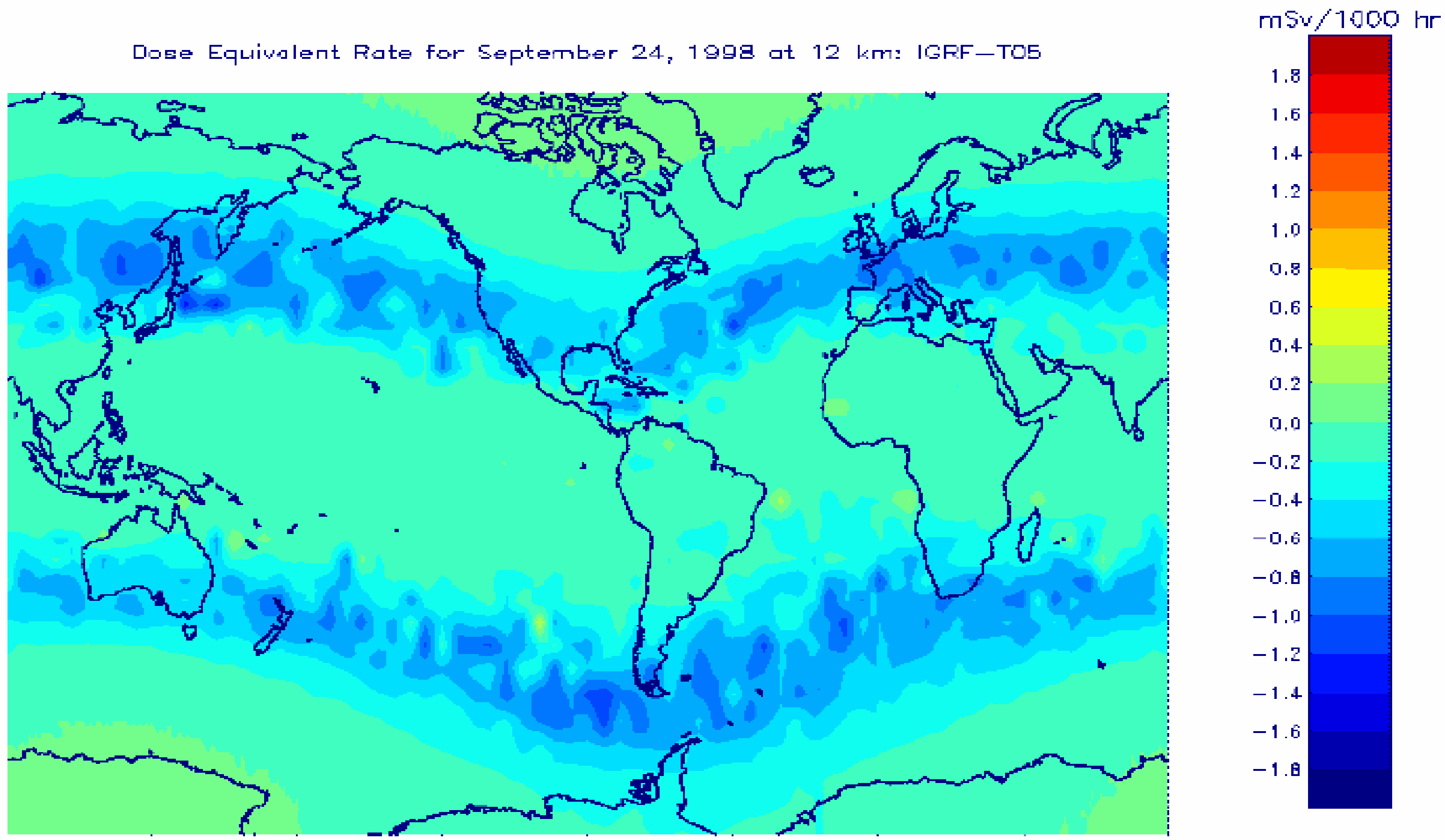

Difference in dose equivalent rate (mSv/1000 hr) at 12 km as a result of using the different magnetic field models in the calculation of vertical geomagnetic cutoff rigidity (i.e., IGRF-T05; see previous Figure).

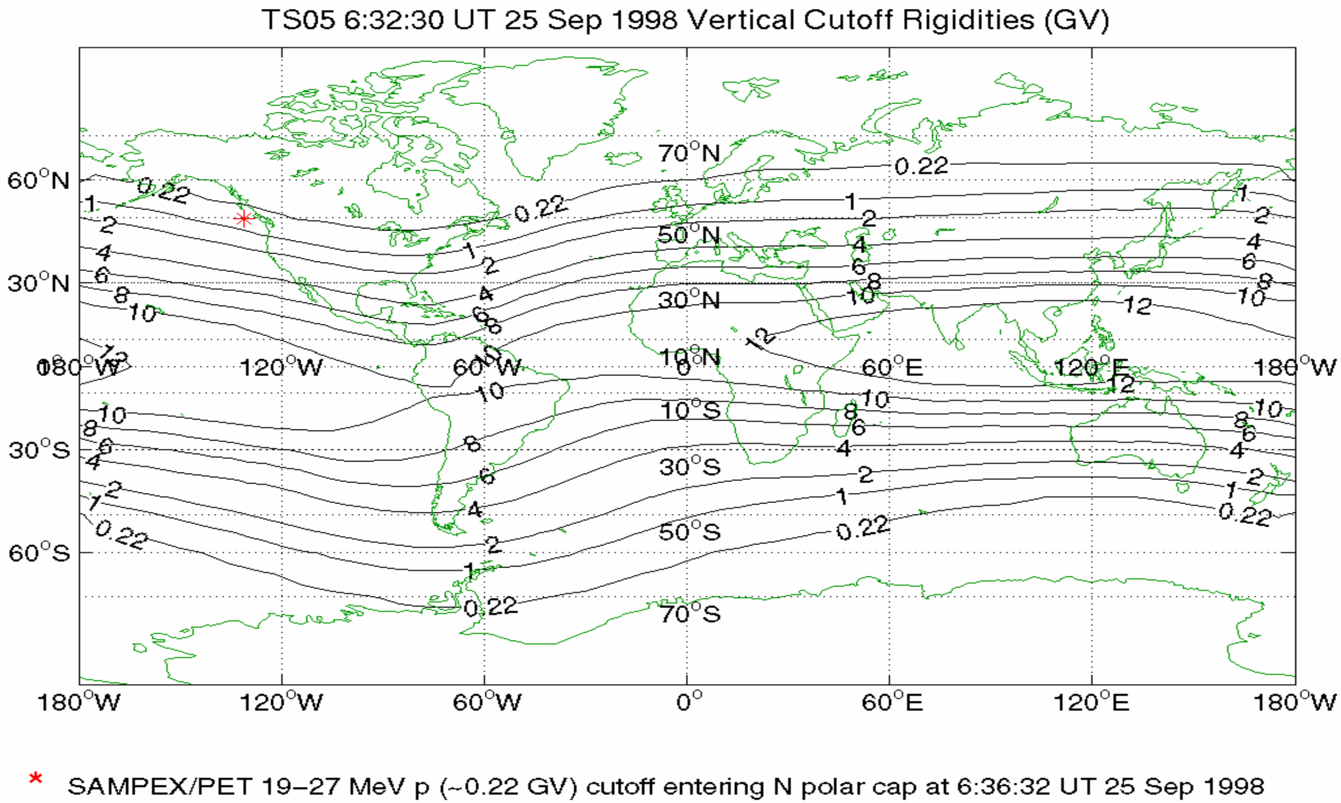

Geomagnetic cutoff rigidities (GV) computed using the T05 magnetospheric magnetic field model for the snap shot at 06:32 UT on September 25, 1998. This snap shot corresponds to the peak solar wind dynamic pressure and minimum Dst-index during this storm period. The SAMPEX observation of cutoff rigidity is shown for the closest time coincidence to the simulated snap shot.

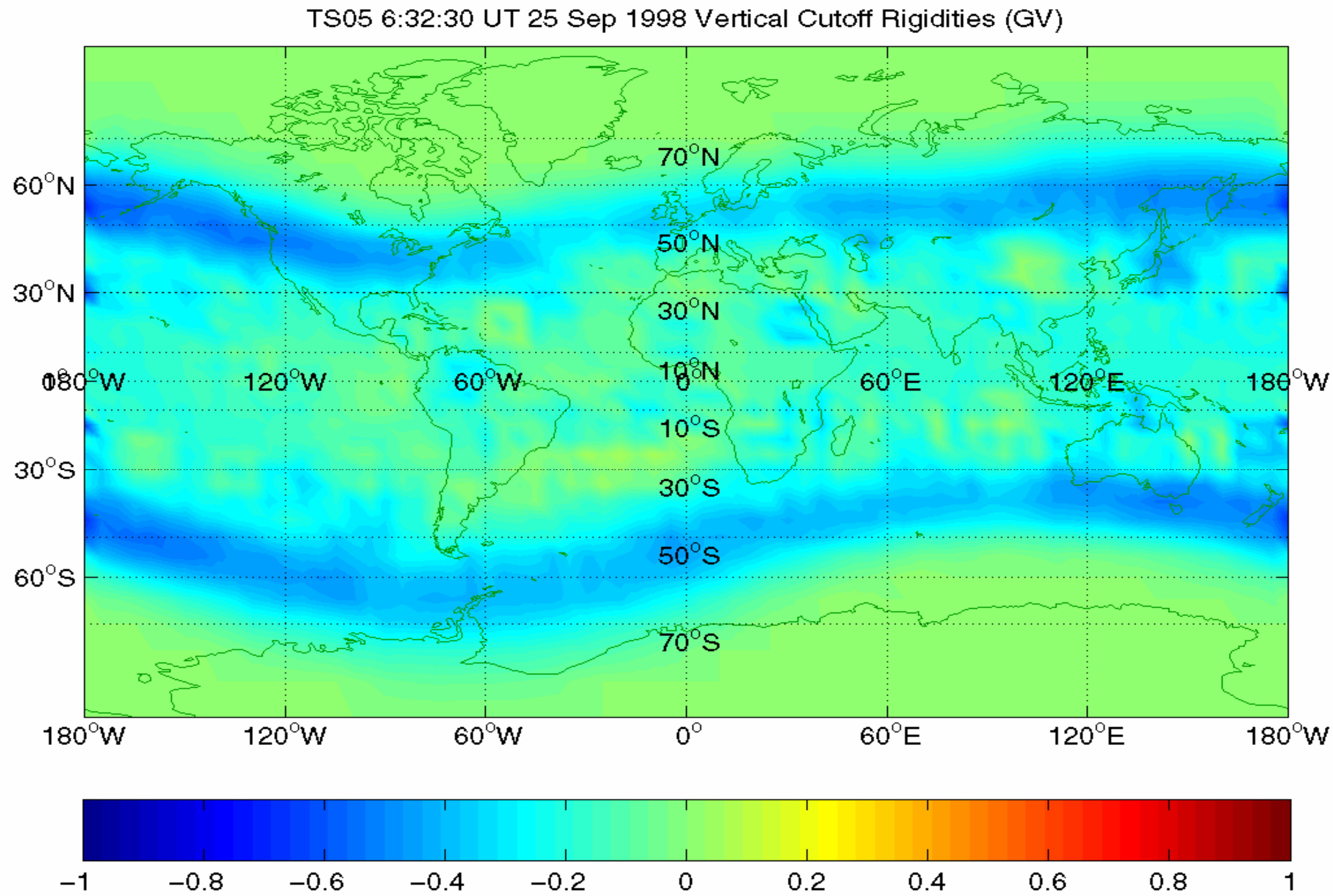

Storm-quiet geomagnetic cutoff rigidity (GV) computed using the T05 magnetospheric magnetic field model. The storm time snap shot corresponds to the same time as Figure 31.